Regional amplification of projected changes in extreme temperatures strongly controlled by soil moisture-temperature feedbacks

M. M. Vogel[1] (iD), R. Orth[1] (iD), F. Cheruy[2] (iD), S. Hagemann[3] (iD), R. Lorenz[1,4] (iD), B. J. J. M. van den Hurk[5], and S. I. Seneviratne[1] (iD)

[1]Institute for Atmospheric and Climate Science, ETH Zürich, Zurich, Switzerland, [2]LMD/IPSL, Université Pierre et Marie Curie, Paris, France, [3]Max Planck Institute for Meteorology, Hamburg, Germany, [4]ARC Center of Excellence for Climate System Science and Climate Change Research Center, University of New South Wales, Sydney, New South Wales, Australia, [5]Royal Netherlands Meteorological Institute, De Bilt, Netherlands

Abstract Regional hot extremes are projected to increase more strongly than global mean temperature, with substantially larger changes than 2°C even if global warming is limited to this level. We investigate the role of soil moisture-temperature feedbacks for this response based on multimodel experiments for the 21st century with either interactive or fixed (late 20th century mean seasonal cycle) soil moisture. We analyze changes in the hottest days in each year in both sets of experiments, relate them to the global mean temperature increase, and investigate processes leading to these changes. We find that soil moisture-temperature feedbacks significantly contribute to the amplified warming of the hottest days compared to that of global mean temperature. This contribution reaches more than 70% in Central Europe and Central North America. Soil moisture trends are more important for this response than short-term soil moisture variability. These results are relevant for reducing uncertainties in regional temperature projections.

1. Introduction

Climate change caused by anthropogenic greenhouse gas emissions is often characterized in the public discourse by the associated increase in global mean temperature. However, for society, economy and stakeholders, regional impacts, and changes in extremes such as heat waves, droughts, or floods are generally of most relevance [e.g., *Field et al.*, 2014; *Vasseur et al.*, 2014]. It is thus essential to communicate the actual regional implications of a given global temperature target [*Seneviratne et al.*, 2016, hereafter S16]. This is particularly important because carbon emissions associated with a mean global temperature rise of 2°C can lead to much stronger temperature increase of hot extremes in land regions (S16).

Many processes contribute to this identified discrepancy between the warming of the global mean temperature and that of regional temperature extremes. We differentiate here among three effects: (i) land mean temperatures are more strongly increasing than global mean temperatures, (ii) several mid-latitude and high-latitude land regions display an additional increase of mean temperature, and (iii) extreme temperatures tend to increase more strongly than mean temperatures in those regions as well. These phenomena can be explained by various mechanisms. For all three aspects, feedback mechanisms are highly relevant, in particular soil moisture-temperature feedbacks in mid-latitude regions [*Seneviratne et al.*, 2010; *Whan et al.*, 2015], and snow- and ice-temperature feedbacks in high-latitude regions [*Hall and Qu*, 2006; *Serreze and Barry*, 2011]. These mechanisms include feedback loops as the (dry) soil moisture and (low) snow/ice anomalies influencing the regional temperature response can themselves be a result of the regional temperature increase. However, temperature and soil moisture changes can also be influenced by other factors such as changes in precipitation. Besides effects of feedbacks with soil moisture and snow, the mean land-sea contrast (mechanism (i) above) is also influenced by the differing heat capacities over land and oceans and differing changes in the lapse rates [*Joshi et al.*, 2008; *Byrne and O'Gorman*, 2013; *Sutton et al.*, 2007].

In mid-latitude regions, the particular strong temperature increase of hot extremes is mostly related to soil moisture-temperature feedbacks as shown in several modeling studies [*Seneviratne et al.*, 2006; *Diffenbaugh and Ashfaq*, 2010; *Seneviratne et al.*, 2013; *Lorenz et al.*, 2016]. Observational studies have also highlighted the relevance of these feedback mechanisms for the development of hot extremes, although generally on interannual time scale rather than for long-term trends [*Hirschi et al.*, 2011; *Mueller and Seneviratne*, 2012;

Miralles et al., 2014]. The strength of this coupling depends on the prevailing climate regime [*Koster et al.*, 2004; *Seneviratne et al.*, 2010]. In a wet climate regime, evapotranspiration is energy limited and thus mostly governed by temperature and radiation (and not soil moisture). In dry regimes, evapotranspiration is very sensitive to soil moisture but the soil moisture variability is too small to affect surface fluxes. Impacts of soil moisture on surface climate are strongest in transitional climate regimes between dry and wet climates, in which evapotranspiration is dependent on soil moisture, while the water availability and variability are large enough to substantially affect the surface fluxes [*Koster et al.*, 2004; *Seneviratne et al.*, 2010]. During summer and/or heat waves, the usually wet regime in regions such as Central Europe and Central North America can temporarily shift toward a soil moisture-limited transitional regime such as the one prevailing in the Mediterranean region [*Seneviratne et al.*, 2006; *Teuling et al.*, 2009; *Seneviratne et al.*, 2010]. In the context of climate change projections, there can be a permanent regime shift from the humid to transitional regime if a region experiences an important mean soil drying, a feature found in several mid-latitude regions and in particular in Central Europe [*Seneviratne et al.*, 2006, 2013]. Temperature projections in regions with a transitional climate regime or displaying shift to this regime exhibit particularly large uncertainties [*Seneviratne et al.*, 2012; *Cheruy et al.*, 2014; S16], which is thus likely related to processes associated with soil moisture-temperature feedbacks. Possible explanations for this large spread have been proposed related to (i) modeling uncertainties in capturing the transition between radiation-limited and soil moisture-limited regimes [*Seneviratne et al.*, 2006; *Boe and Terray*, 2008] and (ii) uncertainties in the projections of future soil moisture trends [*Lorenz et al.*, 2016]. In addition, there is evidence of possible systematic biases in the representation of the soil moisture-temperature coupling and associated processes in current models [*Cheruy et al.*, 2014; *Mueller and Seneviratne*, 2014]. This underlines the importance of understanding land-atmosphere interactions in nature as well as of carefully assessing its representation in climate model projections.

To systematically study the link between soil moisture-climate feedbacks and projected changes in temperature and precipitation [*Intergovernmental Panel on Climate Change*, 2013; *Orth et al.*, 2016], a multimodel experiment with several Earth System Models (ESMs) was performed to investigate the impact of soil moisture-climate feedbacks in projections of the Coupled Model Intercomparison Project Phase 5 [CMIP5; *Taylor et al.*, 2012] (GLACE-CMIP5) [*Seneviratne et al.*, 2013, hereafter S13]. S13 found a drying trend of soil moisture in several regions across the participating models, and resulting substantial effects of these mean soil moisture changes for changes in summer and extreme temperatures, in particular in the Mediterranean region. Recent studies also provided further analyses of the GLACE-CMIP5 experiments [*Berg et al.*, 2015, 2016; *May et al.*, 2015; *Lorenz et al.*, 2016]. In particular, *Lorenz et al.* [2016] focused on the influence of soil moisture on climate extremes.

In this study we assess the relevance of the soil moisture-temperature coupling and its underlying processes for the regional amplification of the increase of extreme temperatures. We focus on regions in which uncertainties in projected changes in extreme temperatures are high and for which the understanding of underlying processes is important for the interpretation of climate projections. We thereby separate and contrast the contributions of the soil moisture-temperature coupling versus that of the globally averaged warming trend based on a multimodel analysis using the GLACE-CMIP5 simulations. Relating projected extreme temperature at the regional scale to global mean temperature increase for these simulations allows us to quantify the contribution of soil moisture-climate feedbacks to the regional amplification of extremes.

2. Models and Methods

2.1. Experiments

We analyze output from five ESMs (see Table S1 in the supporting information) which contributed to the GLACE-CMIP5 project (S13). We employ two GLACE-CMIP5 experiments performed with all models: (i) the CMIP5(-like) reference simulation (hereafter referred to as CTL) and (ii) simulations with prescribed twentieth century soil moisture conditions ("expA" in S13, hereafter referred to as "SM20c") to suppress the impact of soil moisture-climate feedbacks in the projections with a focus on long-term (multidecadal) changes in soil moisture. Note that also short-term and interannual soil moisture feedbacks are disabled in the SM20c setup, although the dominant signal is resulting from the removed long-term soil moisture trend (see hereafter). The CTL simulations were recomputed with prescribed sea surface temperatures (SSTs), sea ice, land use, and the CO_2 concentrations of the corresponding CMIP5 simulation; only for one model (CCSM4) the CTL

simulation is identical to the respective CMIP5 simulation (i.e., fully coupled) (see S13 for details). The SM20c simulations were computed with an identical setup, except for the prescription of the mean 1971–2000 seasonal soil moisture cycle from the CTL simulation of the respective model. Note that prescribing SSTs in the models inhibits a response of the ocean to soil moisture changes; however, these effects are expected to be small [*Orth and Seneviratne*, 2017]. All simulations cover the time period 1951–2100 using historical forcing until 2005 and forcing from a business-as-usual high-emission scenario afterward (Representative Concentration Pathway 8.5) [*Meinshausen et al.*, 2011]. *Lorenz et al.* [2016] added the ACCESS model to the GLACE-CMIP5 ensemble. Since there are a few deviations of the described experimental setup in these simulations (see Text S1), we did not include this model in our main analysis. However, we performed the analyses both with and without the ACCESS simulations. The results are not affected qualitatively, except to some extent in Central North America (see Figures S2 and S7).

The SM20c experiment removes the projected long-term drying of soil moisture as well as the short-term soil moisture variability (other than a climatological annual cycle). Hence, the differences in climate between CTL and SM20c are due to (a) the removed soil moisture trend (i.e., the removed impact of soil moisture-climate interactions at multidecadal time scales) and (b) the removed short-term soil moisture-climate interactions (at subseasonal and interannual time scales). In order to assess the relative importance of (a) and (b), we also consider another experiment from the GLACE-CMIP5 ensemble ("expB" in S13, termed "SMnoVar" hereafter), in which the seasonal cycle of soil moisture is prescribed using a transient 30-year running mean climatology from CTL (S13). Consequently, in experiment SMnoVar only the short-term soil moisture variability (process (b) above) is removed, while long-term trends in soil moisture (a) are still included.

2.2. Extreme Temperatures

To capture future changes in extreme temperatures, we focus on the yearly maximum of daily maximum 2 m air temperatures (hottest day of a year, TX_X), which is a well-established heat index [e.g., *Zhang et al.*, 2011].

We calculate TX_X from daily maximum temperature data at each grid cell and for each model over land only. Note that the resulting TX_X values occur on different days at different locations in different models. We regrid the resulting TX_X fields by bilinear interpolation on a common $2.5° \times 2.5°$ grid. Thereafter we compute multimodel means and subsequently spatial averages across different regions as determined in *Seneviratne et al.* [2012]. For the calculation of spatial mean temperatures, we apply an area-based weighting to account for larger grid boxes toward the equator. In our analysis, we assess TX_X changes over land between the late 21st century (2081–2100) and the historical period (1951–1970) and analyze differences between the SM20c, SMnoVar, and CTL experiments.

In order to compare regional versus global future temperature increase and to compute the additional regional temperature increase, we relate temperature changes in different regions to global mean temperature changes as introduced by *Seneviratne et al.* [2016]. Global mean temperatures are obtained by computing annual means from monthly 2 m temperatures. All temperature anomalies are calculated as 20-year running means from 1971–1990 to 2081–2100, whereas the reference period for inferring changes over time is the 20-year mean between 1951 and 1970. We note that the global warming that was already reached by that time period compared to pre-industrial conditions needs to be accounted when comparing these values to the so-called 1.5C° or 2°C "global warming targets". While the 20-year time window is admittedly an arbitrary choice, we note that slightly different time windows (e.g., 10 years) yield qualitatively similar results (not shown).

2.3. Regions

Beyond global averages we are focusing on five regions out of the large-scale regions defined in *Seneviratne et al.* [2012]. We selected these regions as they (i) exhibit strong changes in the hottest days (Figure 1) and (ii) span different continents and climate regimes: Amazonia (AMZ), Central Europe (CEU), Central North America (CNA), Northern Australia (NAU), and Southern Africa (SAF).

3. Results

3.1. The Role of Soil Moisture for Projected Changes in TX_X

We find that the multimodel mean of TX_X is increasing globally in both experiments (CTL and SM20c) until the end of this century. The projected changes are markedly more pronounced in CTL, with regional increases of
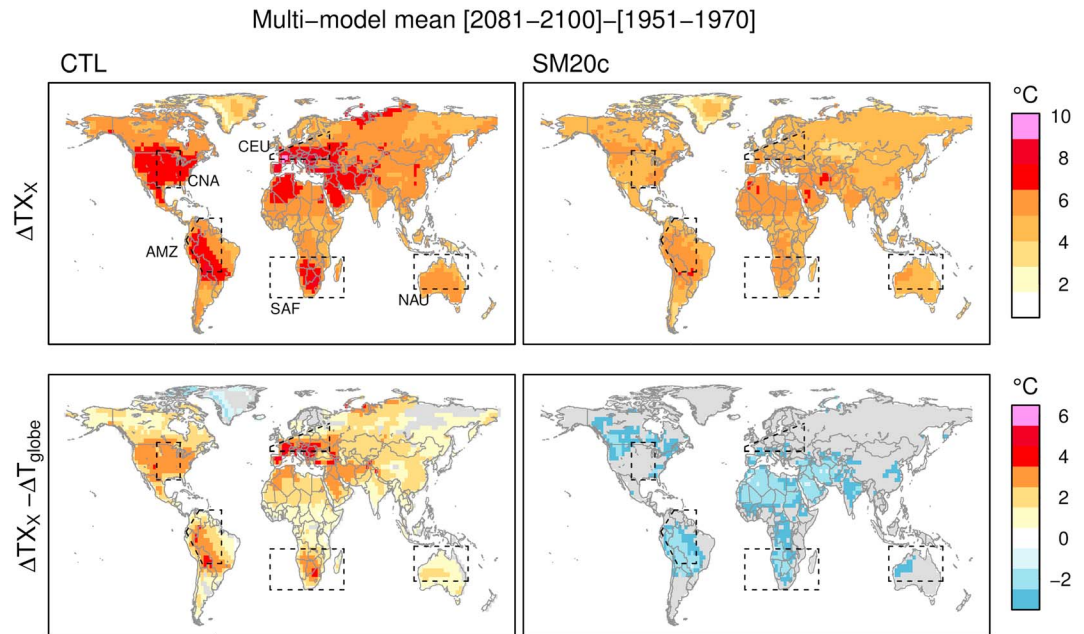
Figure 1. Projected changes in TX_X (top row) between 2081–2100 and 1951–1970 and additional increase of TX_X versus T_{globe} (bottom row) between 2081–2100 and 1951–1970 for CTL (left) and SM20c (right). Grey color denotes insufficient model agreement; i.e. fewer than four of the five models show the same sign of the change. The upper color bar corresponds to Figure 1 (top row), the lower color bar to Figure 1 (bottom row).

up to 10°C, whereas in SM20c temperature changes vary only between 1°C and 6°C (Figure 1, top row). We identify largest regional differences between the projected TX_X increase in CTL and SM20c in AMZ, CEU, CNA, and SAF, as well as in NAU. These large differences indicate that soil moisture-climate feedbacks strongly contribute to future changes in extreme temperatures in these regions.

To compare the role of soil moisture feedbacks associated with (a) long-term (multidecadal) soil moisture trends with (b) the short-term (subseasonal and interannual) variability of soil moisture for changes in extreme temperatures, we also analyze results from the SMnoVar experiment (Figure S1, left). In contrast to the response in SM20c, we find in SMnoVar strong projected changes in TX_X. These results show that most of the impact of soil moisture-climate feedbacks on the projected changes in temperature extremes is associated with the long-term trend in soil moisture rather than short-term soil moisture variability (e.g., concurrent occurrence of dry and hot conditions due to the driving atmospheric conditions or short-term feedbacks).

To identify the amplification of the warming of regional temperature extremes beyond global mean temperature rise, we calculate differences between projected changes in TX_X and projected global mean temperature (T_{globe}) anomalies at each grid cell (Figure 1, bottom row). Note that only robust differences are shown for which at least four out of the five models show the same sign of change. We find a similar spatial pattern as in the top plot, with the same regions exhibiting strongest changes in temperature deviations between CTL and SM20c. Robust signals in the SM20c experiment are only found in South America, Northern America, and large parts of Africa. Some of these regions are in a soil moisture-limited dry regime already in present climate [*Seneviratne et al.*, 2010]. Again, SMnoVar shows similar results to CTL indicating the dominating role of long-term soil moisture trends (compared to that of short-term soil moisture variability) for changes in extreme temperatures (Figure S1, right).

3.2. Regional Amplification

We relate regional TX_X changes until the end of the century to global mean temperature increase in Figure 2 (as in S16). Temperature anomalies refer to 20-year running means starting from the time window 1971–1990 to 2081–2100, always with respect to the base period 1951–1970 (see section 2.2). We show changes for the five selected regions (see section 2.3.) indicated in Figure 1. The ensemble means and the range, defined as
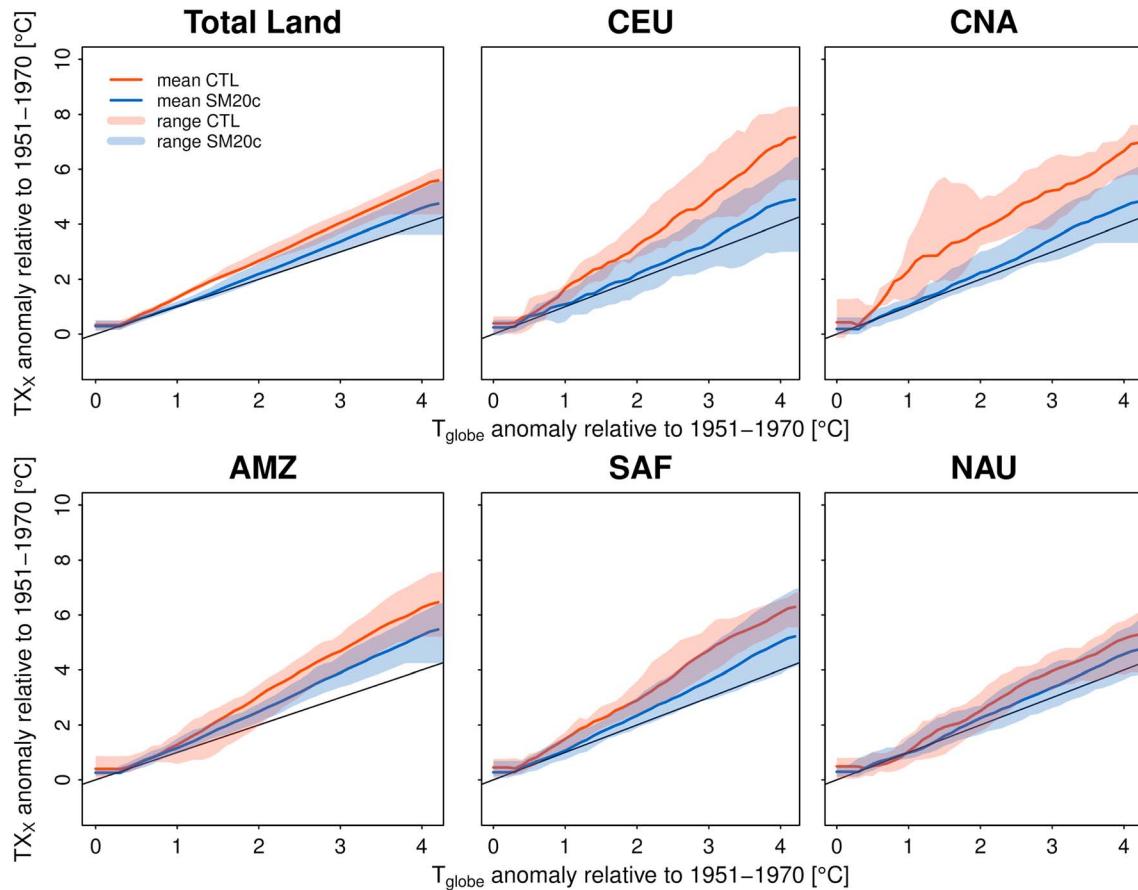
Figure 2. Land TX_X/regional TX_X anomalies versus global mean temperature anomalies. The solid lines are the multimodel mean of CTL (red) and SM20c (blue). The range presents the minimum and maximum values of the individual models in CTL (red shading) and SM20c (blue shading). The identity line indicates identical TX_X anomaly and T_{globe} anomaly increase (black). Anomalies are calculated as 20-year running means from 1971 to 2100 relative to the base period of 1951–1970. Note that the global warming already reached by 1951–1970 needs to be accounted when comparing the values of the x-axis to the so-called 1.5°C or 2°C "global warming targets".

minimum and maximum values from the five models, are computed for CTL (red) and SM20c (blue) separately. The identity line indicates identical TX_X and T_{globe} increases, which is interpreted here as no amplification of regional temperature extremes.

There are clear regional differences both in the magnitude of the amplification of temperature extremes as well as in the spread between the models. For larger global mean temperature anomalies, the model spread is overall increasing, which can be associated with larger uncertainties in the projected future climate.

We find an amplification of TX_X changes with respect to T_{globe} changes in all five regions in CTL as slopes of the multimodel mean are larger than 1. In particular, in CEU the TX_X anomalies are very large, reaching approximately 8°C by the end of the 21st century. Also, in AMZ and CNA multimodel mean anomalies are reaching about 7°C. In SM20c there is only little amplification of TX_X changes in CEU, CNA, and NAU such that the TX_X increase is similar to the T_{globe} increase. The largest deviations between CTL and SM20c are found in CEU and CNA with maximum differences between 2 and 4°C. In SMnoVar the amplification of TX_X with respect to T_{globe} is similar to that in CTL (Figure S3).

These results suggest that soil moisture-temperature feedbacks associated with long-term soil moisture trends are responsible for a large part of the amplification of regional changes in TX_X versus T_{globe} changes, and that these feedbacks contribute strongly to the increase of hot extremes in regions experiencing a drying trend in climate projections. Especially in regions where the evaporative regime varies between energy- and water-limited conditions (such as CEU), this drying has a particularly large impact. This is because a soil moisture drying can cause a shift from a predominantly wet to a predominantly transitional evaporation
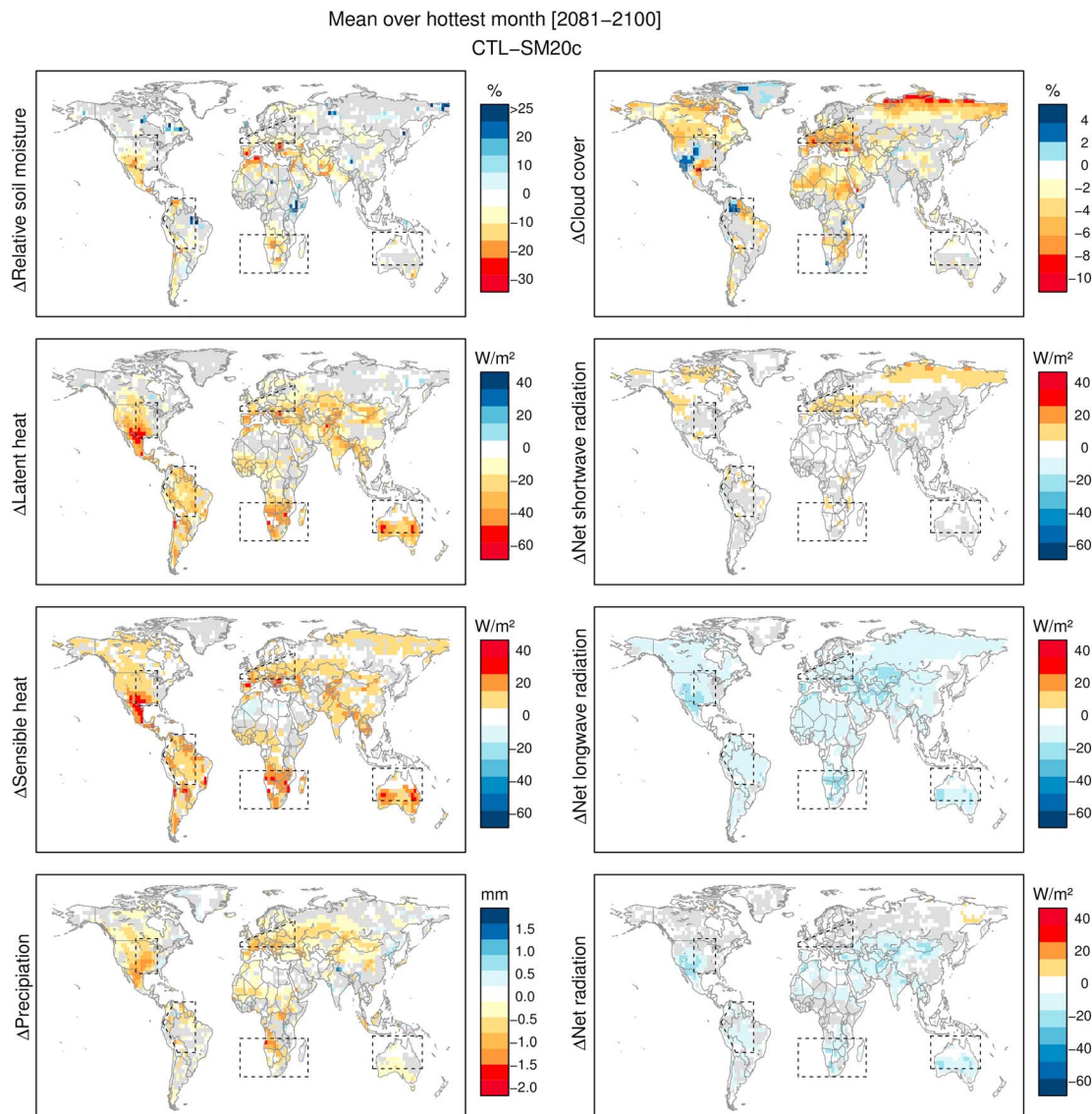
Figure 3. Differences between CTL and SM20c for future changes (2081–2100) of soil moisture, latent heat, sensible heat, precipitation, cloud cover, shortwave, longwave, and net radiation in the three hottest consecutive months (see Figure S5). Relative soil moisture is computed as change between CTL and SM20c divided by SM20c. Grey color denotes insufficient model agreement; i.e., fewer than four of the five models show the same sign of the change.

regime, which enhances the sensitivity of evapotranspiration and consequently temperature to soil moisture [e.g., *Seneviratne et al.*, 2010].

To illustrate the three effects leading to regional amplification of extremes as described in the section 1, we consider also changes in mean temperatures (Figure S4). We find that in most models there is only a minor additional warming of mean land temperature with respect to the global mean temperature if soil moisture feedbacks are disabled (Figure S4a, right). Hence, soil moisture feedbacks play a role in all three components contributing to the additional warming of regional land-based temperature extremes, but in varying degrees: (i) It has some (minor) effect on the increased land-sea temperature contrast, (ii) it leads in some regions to a marked additional mean temperature increase, and (iii) it is found to specifically enhance the temperature increase of hot extremes beyond mean temperature in most of these regions, such as in CEU.

3.3. Processes Leading to Regional Amplification of Temperature Extremes

We provide here an analysis of the physical processes through which soil moisture-temperature feedbacks amplify temperature extremes. For this purpose, we focus on projected changes in soil moisture, latent heat
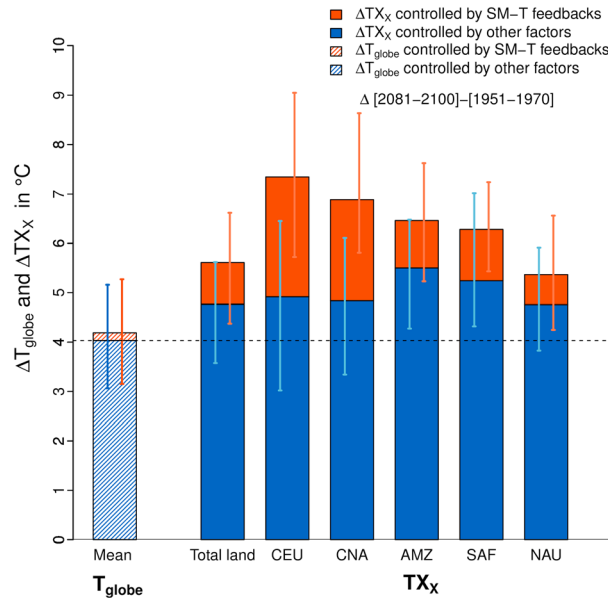
Figure 4. Projected change in global mean temperature (left) and in total land and regional TX_X (right) between 2081–2100 and 1951–1970 due to soil moisture-temperature feedbacks (red) and other factors (blue). The range is determined as minimum and maximum values from the model ensemble.

flux, sensible heat flux, precipitation, cloud cover, and shortwave, long-wave, and net radiation in the hottest months (Figures 3 and S6). We compute three consecutive hottest months using monthly mean temperatures from 1951 to 1970 from each model simulation (Figure S5). In CTL we find decreased summer soil moisture compared with SM20c, which induces decreased latent heat flux in our focus regions. Correspondingly, the sensible heat flux in summer is overall increased in CTL, leading to warmer temperatures. In line with the decreased latent heat flux, we also find a tendency for decreased precipitation and a corresponding decrease in cloud cover in CTL, in particular in CEU. In response, we find increasing net shortwave radiation (i.e., leading to an additional increase of temperature) but decreasing net longwave radiation

(counteracting the previous effect). Overall, the effect on net radiation is small, with a tendency toward less net radiation in the CTL simulations.

These results show that in addition to the direct effect of soil moisture on the surface energy and moisture fluxes, there are also secondary modifications of cloud cover, radiation, and precipitation, which can affect the surface temperature response. Both effects (i.e., direct impacts on the surface energy balance and secondary responses of atmospheric variables) contribute to the observed soil moisture-temperature feedback, although the effects of the changes in cloud cover, radiation, and precipitation are rather small and can even include negative feedbacks (e.g., net effect on radiation). We note that impacts on circulation patterns could possibly also be relevant [*Koster et al.*, 2014], in particular, since circulation anomalies are a strong driver of extreme heat waves [*Cassou et al.*, 2005]. The differences between SMnoVar and CTL are again less pronounced (Figure S6), thus confirming the dominant role of long-term trends in soil moisture for the overall response.

To determine the total contribution of soil moisture-climate feedbacks to the changes in temperature extremes, we compute projected temperature changes for multimodel mean for T_{globe} and TX_X in CTL and SM20c (Figure 4). The difference between the two experiments (red) expresses the contribution of soil moisture-temperature feedbacks. The increase of T_{globe} is similar for both experiments. This illustrates that soil moisture-temperature feedbacks have a minor effect on Tglobe (ocean + land), despite their large effects on land regions.

For projected average changes in TX_X over the global land area, we find mean temperature differences of more than 1°C, showing that soil moisture-climate feedbacks also have detectable average effects over the continents as a whole, despite the small effect on T_{globe} (i.e., when also including the ocean response). Particularly in mid-latitude regions such as CEU and CNA, the contribution of soil moisture-temperature feedbacks is often stronger than that found for global land TX_X. In AMZ, NAU, and SAF, we find a similar response magnitude as over the total land. The multimodel range varies across the regions.

We finally quantify the overall contribution of soil moisture-temperature feedbacks to the amplification of TX_X beyond T_{globe} in different regions (Figure S8). Note that this does not exclude other processes of being relevant; however, this assessment considers the contribution of soil moisture as a necessary (rather than sufficient) condition to this response (see also, e.g., *Hannart et al.*, 2015 for a discussion of this distinction). We

find that for multimodel means 70% of the additional TX_X increase compared to the global mean temperature is removed in CEU and CNA if soil moisture-temperature feedbacks are disabled (Figure S8). In AMZ, NAU, and SAF, contributions of these feedbacks represent between 43% and 50% of the total signal. The large contributions highlight that soil moisture is an essential control of the amplified temperature increase of hot extremes over land compared to the global mean temperature warming. In particular, in mid-latitude regions such as CEU and CNA the additional projected temperature increase of the hottest days beyond the total T_{globe} rise is strongly affected by the long-term soil moisture drying (by more than 70%), but also, in other regions soil moisture-temperature coupling can account for around half of the additional temperature increase.

4. Conclusions

In this study we use simulations from a multimodel experiment to investigate the role of soil moisture-climate feedbacks for projected changes in regional temperature extremes (TX_X). Our results reveal that the projected regional response of TX_x in several mid-latitude land regions can be decomposed in (i) the mean global warming trend and (ii) an additional temperature increase that is strongly affected by soil moisture-temperature feedbacks. This response is related to projected soil moisture drying (on multidecadal time scale), which is shown to have a stronger effect than short-term (subseasonal, seasonal, or interannual) soil moisture variability. Direct soil moisture effects on the surface energy balance together with secondary impacts on other atmospheric variables (e.g., changes in cloud cover, precipitation) are found to be necessary for more than 70% of the amplified response of regional temperature extremes in CEU and CNA, and between 43% and 50% in AMZ, NAU, and SAF. We note that our findings might be influenced by the choice of models available in the GLACE-CMIP5 experiments, although they are well covering the CMIP5 range.

Given the important role of soil moisture for changes in temperature extremes at the regional scale, our results suggest that the identified substantial uncertainties in projections of regional temperature extremes [*Fischer and Schär*, 2010; *Deser et al.*, 2012; *Seneviratne et al.*, 2012; S16] could be addressed with a better consideration of soil moisture-related processes, either through their impacts on internal climate variability or on intermodel spread. In addition, our findings highlight that the reduction of uncertainties in transient climate sensitivity [e.g., *Otto et al.*, 2013] can only address part of the uncertainties in regional projections of extremes and impacts, while intermodel discrepancies in regional soil moisture-climate feedbacks could be dominant for these projections in several regions.

References

Berg, A., et al. (2015), Interannual coupling between summertime surface temperature and precipitation over land: Processes and implications for climate change, *J. Clim.*, *28*, 1308–1328.

Berg, A., et al. (2016), Land-atmosphere feedbacks amplify aridity increase over land under global warming, *Nat. Clim. Change*, *6*, 869–874.

Boe, J., and L. Terray (2008), Uncertainties in summer evapotranspiration changes over Europe and implications for regional climate change, *Geophys. Res. Lett.*, *35*, L05702, doi:10.1029/2007GL032417.

Byrne, M. P., and P. A. O'Gorman (2013), Link between land-ocean warming contrast and surface relative humidities in simulations with coupled climate models, *Geophys. Res. Lett.*, *40*, 5223–5227, doi:10.1002/grl.50971.

Cassou, C., L. Terray, and A. S. Phillips (2005), Tropical Atlantic influence on European heat waves, *J. Clim.*, *18*, 2805–2811.

Cheruy, F., et al. (2014), Role of clouds and land-atmosphere coupling in midlatitude continental summer warm biases and climate change amplification in CMIP5 simulations, *Geophys. Res. Lett.*, *41*, 6493–6500, doi:10.1002/2014GL061145.

Deser, C., et al. (2012), Communication of the role of natural variability in future North American climate, *Nat. Clim. Change*, *2*, 775–780.

Diffenbaugh, N. S., and M. Ashfaq (2010), Intensification of hot extremes in the United States, *Geophys. Res. Lett.*, *37*, 1–5, doi:10.1029/2010GL043888.

Field, C. B., et al. (2014), Technical summary, in *Climate Change 2014: Impacts, Adaptation, and Vulnerability. Part A: Global and Sectoral Aspects. Contribution of Working Group II to the Fifth Assessment Report of the Intergovernmental Panel on Climate Change*, edited by C. B. Field et al., pp. 35–94, Cambridge Univ. Press, Cambridge, U. K., and New York.

Fischer, E. M., and C. Schär (2010), Consistent geographical patterns of changes in high-impact European heatwaves, *Nat. Geosci.*, *3*(6), 398–403.

Hall, A., and X. Qu (2006), Using the current seasonal cycle to constrain snow albedo feedback in future climate change, *Geophys. Res. Lett.*, *33*, L03502, doi:10.1029/2005GL025127.

Hannart, A., et al. (2015), Causal counterfactual theory for the attribution of weather and climate-related events, *Bull. Am. Meteor. Soc.*, *97*, 99–110.

Hirschi, M., et al. (2011), Observational evidence for soil-moisture impact on hot extremes in southeastern Europe, *Nat. Geosci.*, *4*(1), 17–21.

Intergovernmental Panel on Climate Change (2013), *Climate Change 2013: The Physical Science Basis. Contribution of Working Group I to the Fifth Assessment Report of the Intergovernmental Panel on Climate Change*, edited by T. F. Stocker et al., Cambridge Univ. Press, Cambridge and New York.

Joshi, M. M., et al. (2008), Mechanisms for the land/sea warming contrast exhibited by simulations of climate change, *Climate Dynam.*, *30*, 455–465.

Koster, R. D., et al. (2004), Regions of strong coupling between soil moisture and precipitation, *Science*, *305*, 1138–1140.

Koster, R. D., Y. Chang, and S. D. Schubert (2014), A mechanism for land-atmosphere feedback involving planetary wave structures, *J. Clim.*, *27*, 9290–9301.

Lorenz, R., et al. (2016), Influence of land-atmosphere feedbacks on temperature and precipitation extremes in the GLACE-CMIP5 ensemble, *J. Geophys. Res. Atmos.*, *121*, 607–623, doi:10.1002/2015JD024053.

May, W., et al. (2015), Contributions of soil moisture interactions to climate change in the tropics in the GLACE-CMIP5 experiment, *Clim. Dyn.*, *45*(11), 3275–3297.

Meinshausen, M., et al. (2011), The RCP greenhouse gas concentrations and their extensions from 1765 to 2300, *Clim. Change*, *109*, 213–241.

Miralles, D. G., et al. (2014), Mega-heatwave temperatures due to combined soil desiccation and atmospheric heat accumulation, *Nat. Geosci.*, *7*, 345–349.

Mueller, B., and S. I. Seneviratne (2012), Hot days induced by precipitation deficits at the global scale, *Proc. Natl. Acad. Sci.*, *109*(31), 12,398–12,403.

Mueller, B., and S. I. Seneviratne (2014), Systematic land climate and evapotranspiration biases in CMIP5 simulations, *Geophys. Res. Lett.*, *41*, 128–134, doi:10.1002/2013GL058055.

Orth, R., and S. I. Seneviratne (2017), Variability of soil moisture and sea surface temperatures similarly important for warm-season land climate in the Community Earth System Model, *J. Clim.*, doi:10.1175/JCLI-D-15-0567.1, in press.

Orth, R., J. Zscheischler, and S. I. Seneviratne (2016), Record dry summer in 2015 challenges precipitation projections in Central Europe, *Sci. Rep.*, *6*, 28334, doi:10.1038/srep28334.

Otto, A., et al. (2013), Energy budget constraints on climate response, *Nat. Geosci.*, *6*(6), 415–416.

Seneviratne, S. I., et al. (2006), Land-atmosphere coupling and climate change in Europe, *Nature*, *443*(7108), 205–209.

Seneviratne, S. I., et al. (2010), Investigating soil moisture–climate interactions in a changing climate: A review, *Earth Sci. Rev.*, *99*(3-4), 125–161.

Seneviratne, S. I., et al. (2012), Changes in climate extremes and their impacts on the natural physical environment, in *Managing the Risks of Extreme Events and Disasters to Advance Climate Change Adaptation. A Special Report of Working Groups I and II of the Intergovernmental Panel on Climate Change (IPCC)*, edited by C. B. Field et al., pp. 109–230, Cambridge Univ. Press, Cambridge, U. K., and New York.

Seneviratne, S. I., et al. (2013), Impact of soil moisture-climate feedbacks on CMIP5 projections: First results from the GLACE-CMIP5 experiment, *Geophys. Res. Lett.*, *40*, 5212–5217, doi:10.1002/grl.50956.

Seneviratne, S. I., et al. (2016), Allowable CO_2 emissions based on regional and impact-related climate targets, *Nature*, *529*, 477–483, doi:10.1038/nature16542.

Serreze, M. C., and R. G. Barry (2011), Processes and impacts of Arctic amplification: A research synthesis, *Global Planet. Change*, *77*(1-2), 85–96.

Sutton, R. T., B. Dong, and J. M. Gregory (2007), Land/sea warming ratio in response to climate change: IPCC AR4 model results and comparison with observations, *Geophys. Res. Lett.*, *34*, L02701, doi:10.1029/2006GL028164.

Taylor, K. E., R. J. Stouffer, and G. A. Meehl (2012), An overview of CMIP5 and the experiment design, *Bull. Am. Meteorol. Soc.*, *93*(4), 485–498.

Teuling, A. J., et al. (2009), A regional perspective on trends in continental evaporation, *Geophys. Res. Lett.*, *36*, 1–5, doi:10.1029/2008GL036584.

Vasseur, D. A., et al. (2014), Increased temperature variation poses a greater risk to species than climate warming, *Proc. Biol. Sci.*, *281*(1779), 1–8.

Whan, K., et al. (2015), Impact of soil moisture on extreme maximum temperatures in Europe, *Weather Clim. Extremes*, *9*, 57–67.

Zhang, X., et al. (2011), Indices for monitoring changes in extremes based on daily temperature and precipitation data, *Wiley Interdiscip. Rev. Clim. Change*, *2*(6), 851–870.